12th IEA Heat Pump Conference 2017

Sizing, manufacturing, and testing of an evaporator coil for multiple air-borne heat sources

Thore Oltersdorf*[,a], Clemens Dankwerth[a], Simon Braungardt[a], Dr. Marek Miara[a], Prof. Dr.-Ing. Hans-Martin Henning[a], Lars Heinen[b], Frank Salg[b]

[a]Fraunhofer ISE, Heidenhofstrasse 2, 79110 Freiburg, Germany
[b]Vaillant GmbH, Berghauser Strasse 40,42859 Remscheid, Germany

Abstract

In general there is a huge potential on using multiple heat sources for heat pumps (HPs). But to arrive at concepts which are making sense from a thermoeconomical point of view it is of decisive importance to minimize the development costs to be able to use two heat sources. One approach could be the usage of a typical air-to-water HP and its heat source ambient air together with exhaust air as a secondary heat source. In case of increasing air-tightness of residential buildings ventilation systems are very often installed by default. Thus the development costs to use this secondary heat source can be considered as negligible. In the context of this objective a fin-and-tube heat exchanger was sized as evaporator.

In this work the sizing process for a newly developed refrigerant distributor, the circuitry of this evaporator and testing results are presented. The experimental results comprise the refrigerant and air side maldistribution in case of using ambient air, exhaust air or the combined usage of these two heat sources.

Keywords: evaporator, multi-source, exhaust, ambient, air, fin-and-tube, maldistribution, refrigerant, heat pump, circuitry diagonalization

1. Introduction

HP compact units for ventilated houses especially passive houses are state-of-the-art and are often described in literature [1], [2], [3], [4]. Some of these systems are already designed for the usage of exhaust air as well as ambient air but there are only few systems known on the market which are adapted to be used for heating loads that are beyond passive house standards and there is no available literature for these larger system setups available. In the frame of the national-funded project MOSKWA one of the topics was to investigate two sources which are selected out of a nine different heat sources. Based on a potential analysis and due to economic constraints both exhaust air and ambient air are selected as best candidates.

2. Evaporator design

To maximize the evaporator's cooling capacity-reducing problems needs to be addressed during the design process. Main and common problems are listed in Table 1. The integration of ambient air as well as exhaust air into one compact unit results in flow fields with inhomogeneous distribution of temperature as well as humidity.

Table 1: Common capacity-reducing phenomena in evaporators

Capacity reducing phenomena	Level of impact	Countermeasures during

* Corresponding author. Tel.: +49 (0) 761/ 4588-5239.
E-mail address: thore.oltersdorf@ise.fraunhofer.de.

		manufacturing
Frost	High	Not possible
Oil wetting of inner surfaces	Low	Not possible due to oil discharge of compressor
Maldistribution on air side	High	Possible by circuitry and overall flow design
Maldistribution on refrigerant side	Relatively low	Possible by distributor design

To cope with maldistribution specific measures were considered for its compensation. The air side maldistribution is considered by a geometry which maximizes the thermal communication per circuit within the cross sectional area of the air duct just by diagonalization of each circuit. For tubes and the distributor market available specifications were considered as constraints during the sizing process. Fin densities were used as available from manufacturers and wavy fins were used. The sizing was done by using ART (advanced refrigeration technologies) simulation software specialized in vapor compression circuit design [5]. Main objective for the sizing was maximizing capacity for a given construction space by maintaining the needed pressure gradient on the air side. A trivial but important step was maximizing the heat surface area by using 5mm tubes. Since air side maldistribution should be avoided by manufacturing principles, see Table 1, the amount of circuits needed to be increased. On the one side to limit the pressure drop related temperature inhomogeneity on the outer wall surface and on the other side to fulfill the compensation of air side maldistribution due to circuitry diagonalization. The refrigerant side maldistribution was compensated by a specific design for the distributor. To compensate any air side maldistribution a circuitry diagonalization was planned to maximize thermal communication between each circuit and the available cross-sectional area of the air duct but this was not realized for the tested evaporator to allow the indirect analysis of the effective air side maldistribution that takes place by investigating superheat deviations between each refrigerant circuit**.**

The design of the distributor was done by ensuring an annular flow regime for the inlet tube section. The applied flow pattern mapping was developed in [6] and is dedicated to vertical annular (upstream) flows. The inlet tube section was manufactured and assembled with an inner-rifled tube segment to enlarge the probability that the vertical annular flow regime is being stabilized. This could not be sized as before based on flow regimes since there is no vertical upstream flow regime map available that consider inner-rifled tubes in the literature.

Nevertheless this symmetric flow pattern should allow a stable performance of void filling after the liquid film break up behind the nozzle section of the distributor. The optimized 5mm evaporator was simulated based on manufacturer constraints with ART. The selected component had a pressure drop between 1,8kPa and 23.7kPa. For hydraulic balancing the feeder lines were sized with a 2-3 times higher pressure drop based on two-phase pressure drop models from [7] and [8].

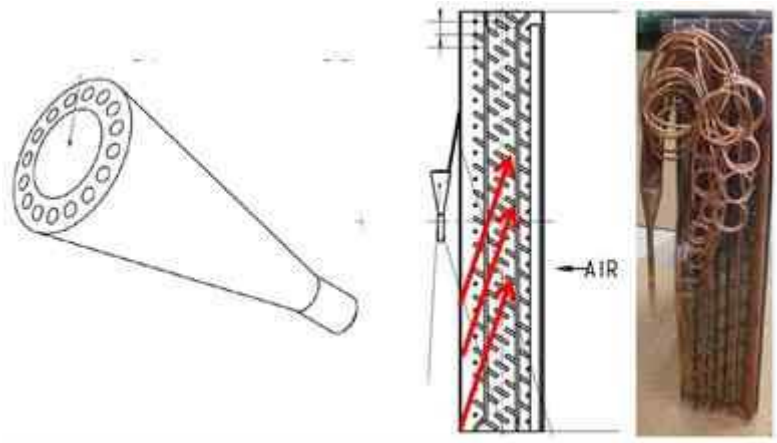


Fig 1. Left picture: Isometric view on the newly sized distributor. Right side: Schematic representation of the circuitry diagonalization planned within the project. The sized, manufactured and assembled distributor as well as the sized feeder lines are shown as well.

3. Test bench setup

At Fraunhofer ISE an air-to-water HP with two different sources were installed. These sources are ambient air and exhaust air of the living area. The modular test bench setup is shown in Figure 2. This test bench uses modules for heat source and heat sink simulation as individual devices to optimize certain individual components of the HP as well as to carry out measurements of the entire system. The entire system is used as air enthalpy based system to fulfill EN 14511 conditions for these types of HPs.

3.1. Test bench configuration

The measurement setup provides various configuration options with different devices. Essentially the measurement setup consists out of an air-to-water HP, a ventilation unit with an optional heat recovery (HR) and a domestic hot water (DHW) storage tank. The used supply units are described below.

The HP as the central device of the setup can either supply the heating circuit or can additionally be connected to the DHW storage tank. The temperature level on the heat sink side can be varied and is dynamically adjustable. On the source side of the HP different configurations can be chosen. The HP can be operated with ambient air only or the ventilation unit can optionally be connected. For the ventilation unit, three settings are feasible. A setup with HR from the exhaust air of the living space or without HR is possible. In both cases the exhaust air is added to the ambient air. In the third case the ventilation unit works as a central ventilation unit. The exhaust air is not added to the ambient air. It is directed outside without any further interaction with the rest of the system. On the source side, the temperature and humidity of the volume flow can be arbitrarily conditioned to imitate different weather scenarios and the behavior of the inhabitants.

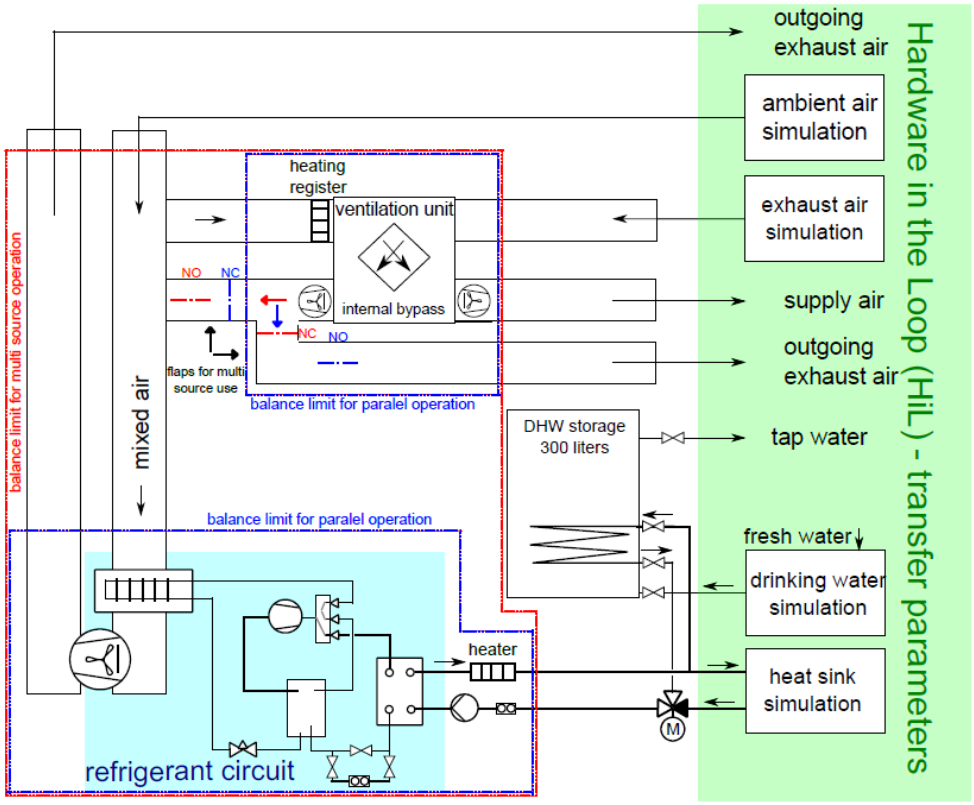


Fig 2. Scheme of the air to water HP system including the ventilation system and domestic hot water preparation.

3.2. Operational description of the test bench

For the experiments described above at the whole four conditioning modules were used. Two modules are dedicated to simulate the heat source and the two other modules to represent the heat sink.

Both heat sources are air-borne which are simulated by precision air conditioning systems to maintain exact control of volume flow, humidity as well as temperature. Pressure at each inlet is controlled via pneumatic flaps

to emulate ambient pressure conditions. This type of flaps allows quickest possible switching between flow configurations to avoid any flows or leakages in unwanted situations i.e. like continuing the air flow during the defrosting process.

The ambient air volume flow is fed directly to the evaporator of the HP as well as to the ventilation unit. The fans of these two air conditioning systems are controlled in order to the demand of volume flow of the HP and ventilation unit.

In the ventilation unit both ambient and exhaust air flow through the cross-flow heat exchanger with or without bypass. In any case the air stream provides the living space with fresh air. From the air conditioning module for the exhaust air, the ventilation unit simulates conditions of the living space. The simulated conditions for temperature and humidity are about 20°C and 50%, respectively. An air volume flow rate of 1200m³/h was maintained in front of the evaporator. This was either reached by ambient air alone or by mixing the two air flows. Depending on the operation mode (cross-flow heat exchanger or bypass) the exhaust air flow is being cooled down or is directly mixed with the ambient air before the mixed air is fed to the evaporator of the HP. As soon as the mixed air has passed the evaporator of the HP, it is referred to as outgoing exhaust air.

On the heat sink side, a DHW module and a module to simulate the heating circuit are used. The DHW module contains a cold water storage, which is kept constantly at 10°C. The module for the heating circuit simulation consists of two water tanks at different temperature levels, a pump and a mixing valve. With the mixing valve and the pump, any volume flow at a certain temperature can be mixed dynamically. The pump of the heating circuit module feds mixed water to a hydraulic switch. With this setup a decoupling of the flows is ensured and standard testing conditions are maintained.

The maldistribution experimental setup was integrated into this test bench by adding an air side temperature sensor array at the inlet and the outlet of the evaporator as well as refrigerant flows. At the refrigerant side each feeder line as well as each entrance into the collecting manifold was connected to a PT100 class A and 1/10B sensors. To ensure thermal communication is dominated at each measurement point thermally conductive paste was used. Each sensor was additionally equipped with thick insulation layer after being connected to the metal surface. Pressure transducers were installed on air and refrigerant side, too. Within the refrigerant lines absolute pressure transducers were installed (0-45bar(abs), Wika). The air side was measured by barometric (Fischer/Meteoclima, Barogeber) and differential pressure measurement (single cell differential pressure transducer, Wika, 0-1000 Pa).

The efficiency analysis for COP determination was realized by using Janitza power analyzers. A/D signal conversion was done either by direct usage of MODBUS compatible sensor devices or by a modular bus systems from Beckhoff with 14-16bit resolution.

4. Results

4.1. Evaporator model validation

To validate the quality of sizing with ART [5] the evaporator's cooling capacity was tested and compared to simulation results. The results are shown in Figure 3. Due to some experimental constraints it was not possible to test the same set of parameters which was used for sizing the evaporator. But only by changing the input parameters the results were almost precisely be reached as shown in the figure below.

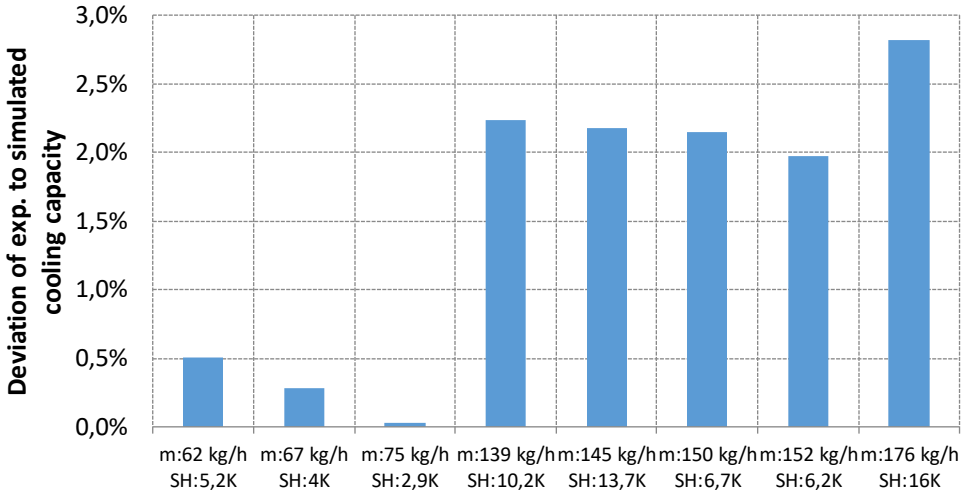


Fig 3. Deviation of simulated and tested capacity of the evaporator.

4.2. Refrigerant side maldistribution

Due to a black-box like control the superheating tested to investigate the refrigerant side maldistribution the superheat could not be hold constant. Based on a comparison of the mean superheat deviations each circuit characteristic can be analyzed, see Figure 4. The enumeration represents the circuits from the top to the bottom. The experiments were done without HR unit operation. Thus there was only simulated ambient air used for the HP operation. In case of a fully symmetrical flow distribution on refrigerant as well as on the air side symmetric conditions should be visible [9]. To compensate for oil solubility and refrigerant property changes and to avoid any confusions due to apparent superheat the superheat values were calculated based on temperature differences and not based on converted pressure-based saturation temperature values. Both methods were compared and apparent superheats determined by pure refrigerant vapor pressure data led to about 10% deviation in superheat measurement with the conventional method.

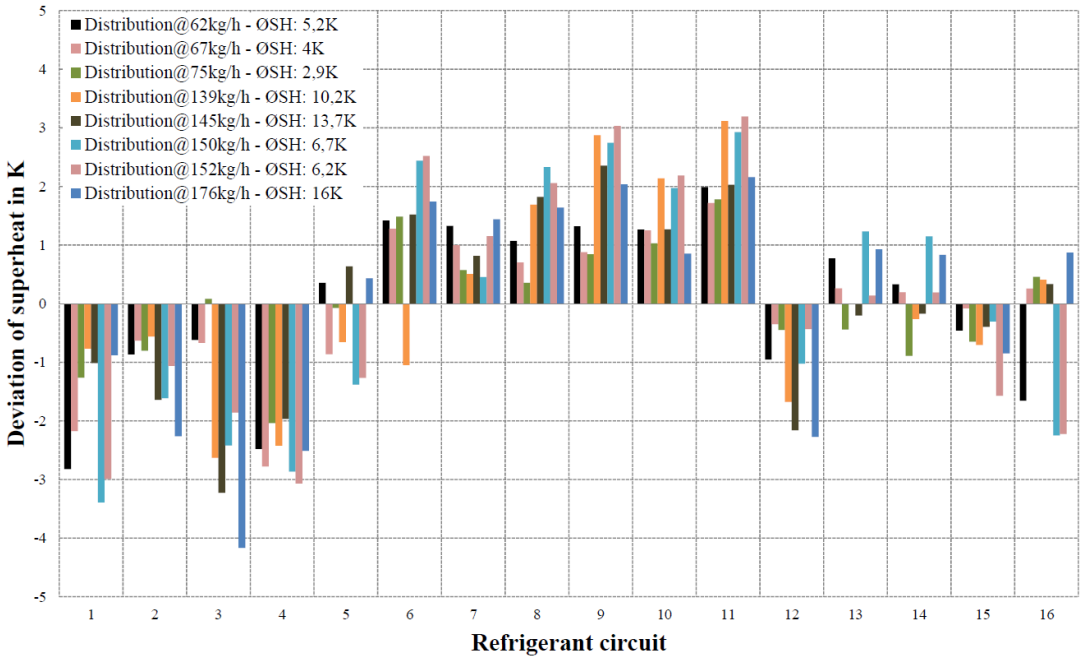


Fig 4. Superheat deviations at each circuit at different mass flow conditions. Bars of the same colour show the difference in relation to the overall superheat per operation condition.

Even though there is no admixture of exhaust air with any lateral impulses into the main air flow a significant unbalance is available within it. Due to the still missing circuitry diagonalization within this prototype heat exchanger the effect of maldistribution can still be studied. Lines 1-5 have clear lower superheat than any mean value indicates. This can either be a superposition of a higher share of liquid refrigerant mass or less thermal communication between these lines and an unbalanced air flow. Lines 6-11 behave more or less normal. This core flow has a higher superheat which indicates a higher share of energy transfer between air side and refrigerant side. The bottom lines 12-16 are closer to the mean value of superheat. Overall this distribution indicates that for higher air volume flows (increasing refrigerant mass flows) there is probably a backflow area within or adjacent to the evaporator in the cross-sectional area of the circuit lines 1-4.

4.3. Admixing of exhaust air with and without HR

As described above, the HP's heat sources are on the one hand ambient air, on the other hand extracted air from the building. The extraction air was not delivered directly to the HP but via a ventilation unit which allows recovering heat from the extracted air by transferring it to the supply air. So, when the extraction air HR is activated, the heat source for the HP is at a lower temperature.

4.4. Air side maldistribution

A grid of temperature sensors was placed before and after the evaporator in order to examine the air side temperature distribution. Figure 5 shows the temperature distribution before and after the evaporator at the tested conditions (A2/W30 and A-7/W34) with and without HR. It is clearly visible that the temperature before the evaporator sinks when activating the HR. Furthermore the warm air from the building is reaching mainly the upper part of the evaporator. This can be explained by the position of the inlet for the extraction air on the upper side to the intake air duct of the HP and by buoyancy forces.



Fig 5. Temperatures before and after the evaporator with extraction air admixing

In the plot of the air temperatures over time (Figure 6) the effect of icing on the temperatures is visible. The frost starts to block the upper part of the evaporator where the moist warm extraction air mainly flows. In this way, the flow resistance is increased there and the warm exhaust air is sucked in by the lower part of the evaporator. After defrosting (approx. minute 100), the initial image is restored, in which the upper temperature sensors receive warm air.



TL01	**TL02**	**TL03**
TL06	**TL05**	**TL04**
TL07	**TL08**	**TL09**

TL12	**TL11**	**TL10**
TL15	**TL14**	**TL13**
TL18	**TL17**	**TL16**

Fig 6. Example of the air temperatures over time at the inlet and outlet oft he evaporator

4.5. Investigation of pressure drop

Studying the pressure drop across the evaporator allows understanding of the dynamic behavior of the frost growth. In Figure 7 this behavior is plotted for the three investigated flow configurations. As can be seen the duration of frost growth on the surfaces is not constant and depends on the flow fed to the evaporator. The relatively dry ambient air with 2°C inlet temperature has the lowest outlet temperature due to the absence of any admixed air flow. Thus it has the lowest temperature level and humidity load, respectively, compared to the other two flow configurations.

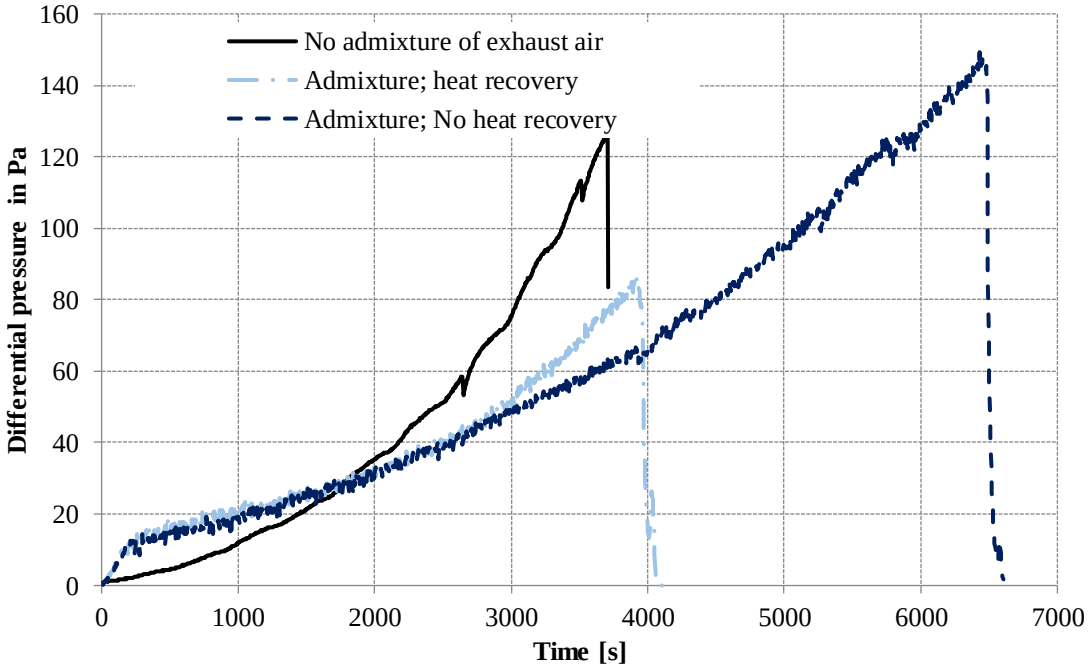


Fig 7. Differential pressure of the evaporator during defrost cycle as a function of time (A2/W30).

The small peaks within the slope of the pressure drop are caused by a pneumatically operated volume flow controls that maintains ambient air pressure at the inlet of the evaporator as well as at the inlet of the HR unit to simulate free suction behavior. The relatively quick increase of the pressure drop in the first 100-200s is caused by condensate retention which re-solidifies to frost again after returning into nominal operation mode. The reason is the usage of an uncoated evaporator in this project period. For the mixed air flow with HR the relatively small peak pressure drop before defrosting is started originates from the interaction of frost control behavior and admixing dynamics and is part of the optimization of the system.

4.6. Energetic evaluation of extracted air admixing

In order to evaluate the energetic effect of extracted air admixing with or without HR in the ventilation unit, for all tests a system COP was calculated consisting in ratio

$$COP_{System} = \frac{Heating\ capacity - Air\ change\ heat\ loss}{Power\ heat\ pump + Power\ ventilation\ unit}$$

The applied system setup can be studied in Figure 2 as well as the balancing limits for efficiency evaluation.

The results are resumed in Table 1. The first column “HP with admixture without HR” represents the extracted air is admixed to the external air as heat source without previous HR. The column “HP with air admixing with HR” shows the results where the extracted air is admixed to the heat source after HR. The column “HP without admixing with HR” shows the results where the ventilation unit is used independent from the HP. In this scenario, the extracted air is released to the outside by a quick switching flap and the HP’s heat source is only outside air.

In the first case "HP with admixture without HR", the exhaust air bypasses the cross-flow heat exchanger in the ventilation unit and is mixed with the ambient air before it is fed to the evaporator of the HP. The second case "HP with admixture with HR" shows the results in which the exhaust air of the living room is cooled down by flowing through the cross-flow heat exchanger in the ventilation unit and is mixed with the ambient air before it is fed to the evaporator of the HP. The last case "HP without admixture with HR " shows the bench mark. In this case the HP and the ventilation unit are operated parallel. The outgoing exhaust air of the ventilation unit is not mixed with ambient air to be fed to the evaporator of the HP. Parallel DHW preparation was prevented.

Table 2: Evaluation of admixture (HP = heat pump; HR = heat recovery)

A2/W30	HP **with** admixture **without** HR	HP **with** admixture **with** HR	HP **without** admixture **with** HR	Percent of ventilation unit related to HP without admixture	Ventilation unit **without** HR	Ventilation unit **with** HR
System COP	**102%**	**115%**	**100%**		Not avail.	Not avail.
Power consumption [W]	92%	96%	100%		1%	2%
Thermal output [W]	94%	111%	100%		-32%	-22%

It can be seen from the table that the benefit of the admixture of exhaust air is depending on the ambient air temperature. At an ambient air temperature of 2°C, an increase of the system COP can be achieved by mixing with exhaust air. This effect is more pronounced when HR in the ventilation unit is activated. Thus less thermal losses have to be compensated.

The comparison between the cases with and without HR in the ventilation unit shows that the COP without HR results in higher system COPs at least for certain operation conditions. This is due to the high temperatures in the exhaust air. As long as the bypass is activated the volume flow of the exhaust air is added with higher temperature and humidity loads, respectively, so that the HP does not run as often into the defrost cycle.

5. Conclusion

A multi-source HP was developed based on the usage of the heat sources ambient air and exhaust air. An evaporator was newly designed by simulation. The device was designed to cope with maldistribution on air and refrigerant side. Subsequently this new evaporator was built and tested for maldistribution. The refrigerant side showed quantifiable backflow areas at the upper half of the evaporator. The air side was tested to analyze the temperature distribution quality as well as the pressure drop development. Results from these experiments are used for optimizing parameters for frost detection and defrosting. Testing at different operation modes and investigating the temperature distribution at the inlet allows identifying regions with stable inlet temperature development.

An exemplary efficiency analysis at A2/W30 shows that there are advantages to do exhaust air admission with HR for certain operation conditions.

6. Outlook

The next step will include the realization of the originally developed circuitry diagonalization as well as hydrophilic coating. A precise flow distribution will be quantified for the air inlet conditions with sub-cm resolution by PIV analysis. The backflow area in the upper half of the duct cross section needs to be investigated to develop appropriate countermeasures for solving this air side maldistribution effect. A fin-staging is discussed to get better countermeasures also for varying

7. Acknowledgements

The authors wish to express their gratitude to the German Federal Ministry of Economics and Technology (BMWi) and Project Management Jülich (PTJ) for funding the joint research project 'MOSKWA' (FKZ 03ET1169B and 03ET1169C). Special thanks also to the colleagues from RWTH Aachen for their cooperation.

References

1. Bühring, A., Jaeschke, M., Bichler, C.: Aktueller Stand der Weiterentwicklung von Lueftungs-Kompaktgeraeten. Energieeffizientes Bauen **6**(4), 3–11 (2005)
2. Zewe, O.: Atmungsaktiv und Kuschelwarm. Die Alleskönner fürs Wohlfühlklima in einer Übersicht. Ein Vergleich aktueller Kompaktanlagen zur Wärmebereitstellung und Lüftung von Passivhäusern. Passivhaus Kompendium **1**(1), 54–61 (2006)
3. Furter, R., Wenger, L.: Kompaktlüftungsgeräte, Prüfreglement, erste Messresultate. In: Tagungsband des 14. Schweizerischen Status-Seminars Energie- und Umweltforschung im Bauwesen, pp. 143–150, ETH Zuerich (2006)
4. Buehring, A.: Theoretische und experimentelle Untersuchungen zum Einsatz von Lueftungs-Kompaktgeraeten mit integrierter Kompressionswaermepumpe. PhD Thesis, TUHH (2001)
5. Corberan, J.M., Gonzalvez, J., Montes, P., Blasco, R.: 'ART' A Computer Code to Assist the Design of Refrigeration and A/C Equipment. In: Proceedings of International Refrigeration and Air-Conditioning Conference, Paper ID 507, Purdue (2003)
6. Hewitt, G.: Churn and Whispy Annular Flow Regimes in Vertical Gas-Liquid Flows. Energy & Fuels **26**(7), 4067–4077 (2012)
7. Friedel, L.: Druckabfall bei der Strömung von Gas/Dampf-Flüssigkeitsgemischen in Rohren. Chemie Ingenieur Technik **50**(3), 167–180 (1978)
8. Mueller-Steinhagen, H., Heck, K.: A simple friction pressure drop correlation for two-phase flow in pipes. Chemical Engineering and Processing: Process Intensification **20**(6), 297–308 (1986)
9. Braungardt, S., Lange, B., Oltersdorf, T.: Experimental Comparison of Different Two-Phase Refrigerant Distribution Devices. In: Proceedings of the IEA Heat Pump Conference 2017, Rotterdam (2017)